Heat Capacities and Derived Thermodynamic Functions of 1-Octadecanol, 1-Nonadecanol, 1-Eicosanol, and 1-Docosanol between 10 K and 370 K

J. Cees van Miltenburg* and Harry A. J. Oonk

Chemical Thermodynamics Group, Debye Institute, Utrecht University, Padualaan 8, 3584-CH Utrecht, The Netherlands

Lourdes Ventola

Dpt. Cristallografia, Universitat de Barcelona, C/Marti i Franquès, S/N-08028 Barcelona, Spain

The molar heat capacities of the linear alcohols 1-octadecanol ($C_{18}H_{38}O$), 1-nonadecanol ($C_{19}H_{40}O$), 1-eicosanol ($C_{20}H_{42}O$), and 1-docosonol ($C_{22}H_{46}O$) were measured from 10 K to 370 K. The derived absolute entropies were fitted as a function of the carbon number (n) in the linear chain. At 360 K the function is $S°(360\ \mathrm{K},n) = \{117.52 + 38.328n\}\ \mathrm{J{\cdot}K^{-1}{\cdot}mol^{-1}}$. A simple function was found for the heat capacity of the liquids. From the melting point to 370 K the liquid heat capacities can be represented within the measuring error with $C_{p,l}(n,T) = \{-450.41 + 36.4968n + 1.47317T\}\ \mathrm{J{\cdot}K^{-1}{\cdot}mol^{-1}}$. The solid−solid phase transition in 1-octadecanol was investigated in more detail, and the relative Gibbs energy curves of both solid phases and the liquid phase are presented.

Introduction

The normal 1-substituted alcohols have received far less interest than the *n*-alkanes. The measurements of thermal properties for the long chain *n*-alcohols published are limited to DSC measurements[1−4] and an adiabatic study of C_{13} to C_{16} 1-alcohols around room temperature.[5] Furthermore, the melting and transition events were studied by X-ray methods,[6−8] dielectric measurements,[9] and direct visual observation in capillary tubes.[10,11] An extensive study of the infrared spectra has been published.[12] We are not aware of high-precision low-temperature studies, which may be used to derive entropy values and other thermodynamic properties.

Compounds containing long aliphatic chains are interesting from different viewpoints. They form important building blocks in paraffins, hydrocarbons, polyethylene, and glycerides. The physical property behavior of these compounds is due to the presence of long aliphatic chains. A review of the physical properties of these molecules can be found in the *Handbook of Lipid Research*.[13] Another more recent aspect of these substances is their potential application in heat storage materials. The alcohols have the advantage of negligible or no subcooling and are not very chemically aggressive. Mixing of different members of the family allows one to manipulate the optimum working temperature for heat storage. Our group works in this field in cooperation with the universities of Bordeaux and Barcelona, organized in the Réseau Européen sur les Alliages Moléculaire (REALM).

Experimental Section

Three compounds were purchased from Fluka Chemica with an estimated purity of better than 98%. The fourth, 1-docosanol was bought from Aldrich with a stated purity of 98%. The compounds were used without further purification. The calorimeter used (laboratory-design indication CAL VII) was home-built as a copy of CAL V.[14,15] Below 30 K, the reproducibility of the calorimeter is about 1%, between 30 K and 100 K, 0.05−0.1%, and above 100 K, 0.03%. The accuracy of the heat capacity measurements

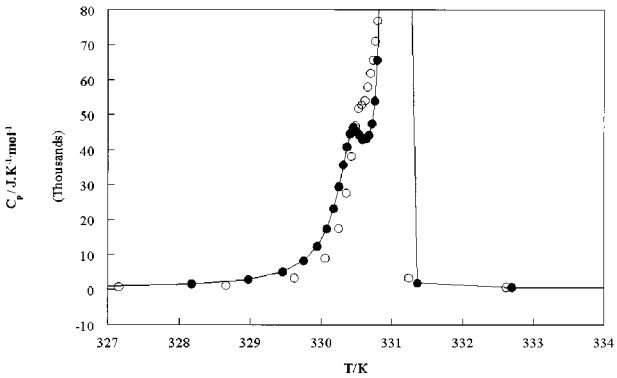

Figure 1. Molar heat capacity of 1-octadecanol around the melting point: ○, material as received; ●, material after being melted in the calorimeter.

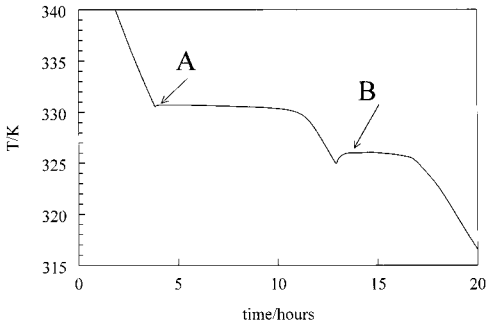

Figure 2. Cooling curve of 1-octadecanol; all four compounds show two thermal events in their cooling curves; A and B indicate the temperatures mentioned in the text.

* Corresponding author. Fax: +31 302533946. E-mail: miltenb@chem.uu.nl.

10.1021/je000048s CCC: $20.00
Published on Web 12/12/2000

Table 1. Experimental Data Series for *n*-Octadecanol

T/K	C_p/J·K^{-1}·mol^{-1}	T/K	C_p/J·K^{-1}·mol^{-1}	T/K	C_p/J·K^{-1}·mol^{-1}	T/K	C_p/J·K^{-1}·mol^{-1}	T/K	C_p/J·K^{-1}·mol^{-1}
series 1		332.61	695.86	52.28	104.36	152.21	264.34	287.35	458.55
296.17	476.27	334.73	698.87	54.86	111.03	154.19	266.67	290.31	465.13
296.97	477.89	336.79	702.14	57.46	117.50	156.17	269.00	293.28	472.36
298.37	481.44	338.77	705.36	60.09	123.77	158.14	271.56	296.24	479.80
300.36	486.75	340.76	708.33	62.75	129.89	160.12	273.71	299.20	487.32
303.72	495.54	342.75	711.55	65.44	135.98	series 6		302.16	495.65
304.50	498.12	344.74	714.82	68.15	141.88	162.00	275.69	305.11	504.47
305.88	502.27	346.73	717.70	70.88	147.63	163.58	277.35	308.06	514.29
307.86	508.78	348.73	720.84	73.63	153.24	165.86	279.79	310.99	525.73
309.84	515.75	350.72	723.56	76.40	158.73	168.82	283.21	313.87	539.58
311.81	523.48	352.71	726.72	79.18	164.09	171.77	286.55	316.70	555.88
313.77	532.13	354.70	729.49	81.98	169.24	174.73	289.99	319.47	580.25
315.74	541.67	356.69	732.26	84.80	174.24	177.68	293.31	322.15	624.69
317.69	552.96	358.71	736.25	87.60	179.18	180.64	296.72	324.66	715.87
319.64	565.97	series 2		90.35	183.77	183.60	300.38	326.83	998.57
321.58	582.92	6.42	1.59	93.03	188.13	186.56	303.74	328.39	1850
323.51	609.33	7.95	2.14	95.64	192.29	189.53	307.28	329.29	3957
325.38	659.88	9.39	3.25	98.20	196.31	192.49	310.88	329.76	7939
327.16	775.60	11.15	4.87	100.70	199.73	195.44	314.44	330.02	13950
328.66	1212.90	12.97	7.29	series 5		198.40	318.02	330.17	21446
329.62	3329	15.00	10.55	95.70	191.77	201.35	321.69	330.28	29319
330.06	9002	17.24	14.47	97.40	194.44	204.31	325.55	330.36	35611
330.25	17524	19.69	19.23	99.22	196.94	207.28	329.16	330.43	38431
330.35	27636	22.27	25.02	101.17	200.68	210.24	333.00	330.50	37905
330.42	38122	24.98	31.63	103.11	203.25	213.21	336.90	330.57	36552
330.48	46830	27.84	38.29	105.06	205.98	216.17	340.68	330.64	39764
330.53	51849	30.66	45.46	107.01	208.90	219.13	344.55	330.71	45596
330.57	52878	33.14	52.64	108.96	211.50	222.09	348.64	330.76	57831
330.61	54121	series 3		110.91	214.17	225.06	352.66	330.80	73374
330.65	58022	5.49	0.18	112.87	216.84	228.03	356.81	330.83	99951
330.69	61894	7.26	1.69	114.83	219.40	230.99	360.95	330.86	117430
330.73	65679	8.43	2.52	116.79	221.97	233.96	365.35	330.88	153761
330.76	71048	10.19	4.00	118.75	224.50	236.92	369.66	330.89	204468
330.79	76858	12.35	6.23	120.71	227.00	239.88	373.97	330.90	266856
330.82	85769	15.48	11.56	122.67	229.47	242.85	378.63	330.91	480056
330.85	94521	15.60	11.58	124.64	231.98	245.81	383.14	330.91	758099
330.87	117629	20.88	21.79	126.60	234.52	248.78	387.73	330.92	760250
330.89	145169	23.34	27.49	128.56	236.79	251.75	392.64	330.92	362245
330.90	168908	26.03	34.23	130.53	239.11	254.72	396.31	330.94	169411
330.92	220591	29.03	41.18	132.50	241.41	257.70	401.47	330.97	61870
330.92	376370	31.81	48.76	134.46	243.84	260.67	406.59	331.77	1312.63
330.93	−823271	series 4		136.44	246.10	263.63	411.89	333.78	697.64
330.92	−4861643	34.02	55.34	138.40	248.36	266.60	417.00	336.23	701.20
330.92	−895038	35.93	60.73	140.37	250.62	269.56	422.35	338.67	704.87
330.92	−742115	40.39	71.49	142.35	253.01	272.52	428.50	341.10	708.60
330.92	−570578	42.48	78.06	144.32	255.41	275.48	433.74		
330.91	−1013209	44.72	83.99	146.29	257.57	278.45	439.39		
330.92	171031	47.23	90.93	148.26	259.81	281.42	445.79		
331.24	3342	49.74	97.70	150.24	262.07	284.38	452.32		

Table 2. Thermodynamic Properties at Selected Temperatures for *n*-Octadecanol (M = 270.4991 g·mol^{-1}, $\Phi^\circ_m \stackrel{def}{=} \Delta_0^T S^\circ_m - \Delta_0^T H^\circ_m/T$)

T/K	$C^\circ_{p,m}$/J·K^{-1}·mol^{-1}	ΔS°_m/J·K^{-1}·mol^{-1}	ΔH°_m/J·mol^{-1}	Φ°_m/J·K^{-1}·mol^{-1}
10	3.8	1.32	9.9	0.33
15	10.55	4.14	45.7	1.094
20	19.90	8.41	120.6	2.378
25	31.68	14.13	250.2	4.126
30	43.66	20.93	437.6	6.345
35	58.18	28.67	689.8	8.967
40	70.44	37.27	1 012	11.96
45	84.76	46.44	1 402	15.27
50	98.38	56.07	1 860	18.87
55	111.40	66.06	2 385	22.70
60	123.55	76.29	2 973	26.74
65	134.99	86.63	3 619	30.95
70	145.80	97.03	4 321	35.30
75	155.97	107.44	5 076	39.76
80	165.63	117.82	5 880	44.32
85	174.59	128.13	6 731	48.94
90	183.20	138.35	7 625	53.63
95	191.27	148.47	8 561	58.35
100	198.38	158.47	9 536	63.11
105	205.90	168.33	10546	67.89
110	212.92	178.07	11594	72.67
120	226.10	197.17	13790	82.26
130	238.49	215.76	16114	91.81
140	250.19	233.87	18557	101.32
150	261.80	251.53	21118	110.74
160	273.27	268.79	23794	120.08
170	284.49	285.69	26582	129.33
180	295.99	302.28	29484	138.48
190	307.91	318.60	32503	147.53
200	320.01	334.70	35643	156.49
210	332.70	350.62	38907	165.35
220	345.74	366.40	42298	174.14
230	359.56	382.07	45824	182.84
240	374.15	397.68	49492	191.46
250	389.51	413.26	53310	200.02
260	405.27	428.84	57282	208.52
270	423.07	444.47	61423	216.97
280	442.53	460.20	65750	225.38
290	463.71	476.10	70282	233.75
298.15	483.07	489.20	74136	240.55
300	487.88	492.21	75033	242.10
310	520.74	508.70	80066	250.43
320	581.29	526.05	85530	258.77
331.2[a,b]	581.2	546.34	91961	268.68
331.2[a,c]	694.51	747.16	158473	268.68
340	707.47	765.54	164642	281.30
350	722.83	786.27	171793	295.43

[a] Extrapolated. [b] Solid. [c] Liquid.

Table 3. Melting Experiments of *n*-Octadecanol[a]

experiment	triple point/K	ΔH_{fusion}/J·mol^{-1}	purity/%	remarks
1	331.12	66 873	98.9	as received
2	331.22	66 733	98.2	
3	331.16	66 643	98.6	
4	331.23	66 601	98.2	slow heating
5	331.20	66 512	98.8	used in Table 2
mean value		66 672 ± 200		

[a] The following linear fits were used for the iterative calculation of the baseline: C_p[solid] = {−374.29 + 2.88485T} and C_p[liquid] = {204.82 + 1.47854T} J·K^{-1}·mol^{-1}.

was checked with *n*-heptane and with synthetic sapphire. No deviations larger than 0.2% from the recommended values were found. The compounds were evacuated for about 0.5 h before closing the measuring vessel. A helium pressure of about 1 kPa was admitted before closing in order to promote the heat exchange within the vessel. Measurements were made in the intermittent mode, using stabilization periods of about 600 s and heat input periods of about 500 s. The temperature increase was generally about 2 to 3 K for each measurement. Each compound was first measured from room temperature up to about 360 K. Then a slow, controlled cooling curve was measured by setting the inner adiabatic shield and the wire heater about 10 K below the temperature of the vessel. This resulted in a cooling rate outside the crystallization area of about 4 K·h^{-1}.

Between 5 K and 30 K, stabilization and input periods of about 100 to 150 s were used. Measurements on 1-octadecanol were made with 6.365 g, on 1-nonadecanol with 3.277 g, for 1-eicosanol with 4.2397 g, and for 1-docosanol with 4.6422 g.

After completion of the measurements, all data were combined in one file. The data consist of the mean tem-

Table 4. Experimental Data Series for *n*-Nonadecanol

T/K	C_p/J·K^{-1}·mol^{-1}	T/K	C_p/J·K^{-1}·mol^{-1}	T/K	C_p/J·K^{-1}·mol^{-1}	T/K	C_p/J·K^{-1}·mol^{-1}	T/K	C_p/J·K^{-1}·mol^{-1}
series 1		349.96	758.48	43.47	83.20	174.01	301.62	305.14	519.19
298.06	493.77	351.94	761.55	45.89	90.05	176.97	305.17	307.10	524.83
298.61	496.47	353.94	764.83	48.34	97.03	179.93	308.77	309.06	530.43
299.89	500.40	355.93	767.20	50.84	103.98	182.89	312.56	311.02	536.05
301.89	505.51	357.92	770.16	53.37	110.96	185.85	316.12	312.97	542.71
303.87	511.60	series 2		55.93	117.96	188.81	319.90	314.92	549.61
305.86	516.69	6.04	1.23	58.53	124.61	191.77	323.50	316.87	557.52
307.85	522.50	8.02	1.77	61.16	131.13	194.74	327.13	318.83	567.19
309.83	528.56	10.11	4.05	63.81	137.65	197.70	330.92	320.77	581.18
311.82	534.96	11.78	6.11	66.49	143.70	200.67	334.74	322.72	591.15
313.79	542.65	13.72	8.94	69.20	149.63	203.63	338.89	324.66	608.25
315.77	549.86	15.95	12.61	71.93	155.57	206.59	342.67	326.58	644.38
317.74	557.94	18.29	17.21	74.67	161.37	209.56	346.62	328.39	816.90
319.71	566.73	20.76	22.19	77.44	166.95	212.53	350.78	329.61	3197
321.68	577.16	23.35	28.30	80.22	172.41	215.49	354.77	330.11	10868
323.64	590.33	26.05	35.26	83.01	177.75	218.46	358.82	330.33	22224
325.60	608.37	28.90	42.05	85.82	182.88	221.43	363.29	330.45	33483
327.54	646.59	series 3		88.68	188.07	224.40	367.30	330.55	41110
329.36	836.40	6.11	0.96	91.51	192.92	227.36	371.74	330.63	41967
330.40	7439	7.66	1.70	94.28	197.53	230.33	376.09	330.73	33889
330.64	25023	9.50	3.32	97.13	202.21	233.29	380.63	330.87	18133
330.75	37370	11.18	4.94	100.02	206.30	236.26	385.18	331.30	4559
330.84	40285	13.14	7.75	series 6		239.23	389.81	332.39	1533
330.93	37242	15.24	11.24	102.65	211.15	242.20	394.70	333.51	4102
331.03	30393	17.50	15.26	104.29	213.75	245.17	399.18	334.01	12024
331.17	21213	19.92	20.31	106.58	217.22	248.14	404.07	334.21	27122
331.40	10928	22.46	26.16	109.48	221.26	251.11	408.83	334.31	45287
331.97	3500	25.11	32.81	112.38	225.43	254.08	413.10	334.38	75965
332.92	2542	27.90	39.32	115.27	229.56	257.05	417.91	334.42	105450
333.72	5856	30.85	47.22	118.17	233.32	260.02	423.17	334.44	156307
334.09	15958	series 4		121.08	237.34	262.98	428.46	334.46	238467
334.26	30569	6.11	0.92	123.99	241.20	265.95	433.51	334.48	330548
334.35	47456	7.91	1.93	126.91	245.25	268.92	438.73	334.49	475173
334.41	68205	9.74	3.55	129.83	248.68	271.88	444.37	334.49	472409
334.46	101334	11.50	5.53	132.76	252.31	274.85	450.07	334.50	288053
334.49	133052	13.54	8.36	135.69	256.11	277.81	455.73	335.07	2374
334.51	177928	15.71	11.94	138.63	259.60	280.78	462.06	336.77	739.51
334.52	−367256	18.01	16.28	141.56	263.25	283.74	468.47	339.06	741.95
334.50	−156428	20.45	21.28	144.50	266.84	286.70	475.09	341.20	745.26
334.49	334341	23.02	27.36	147.44	270.25	289.66	481.30	343.18	748.94
334.54	46982	25.69	34.51	150.38	273.96	series 7		345.17	751.78
335.58	956.92	28.52	40.83	153.32	277.63	291.93	484.38	347.15	754.83
337.74	739.78	series 5		156.27	281.00	293.55	489.64	349.13	757.63
339.95	742.91	32.19	51.86	159.22	284.29	295.34	493.89	351.12	760.66
342.01	745.79	34.08	57.36	162.18	287.84	297.30	498.56	353.10	763.98
344.00	750.39	36.42	63.77	165.13	291.41	299.26	503.27	355.08	766.71
345.98	752.56	38.74	69.20	168.09	294.72	301.22	507.77	357.07	769.71
347.97	755.63	41.09	76.20	171.05	298.20	303.19	514.05	359.06	772.79

Table 5. Thermodynamic Properties at Selected Temperatures for *n*-Nonadecanol (M = 284.5260 g·mol^{-1}, $\Phi_m^\circ \stackrel{\text{def}}{=} \Delta_0^T S_m^\circ - \Delta_0^T H_m^\circ/T$)

T/K	$C_{p,m}^\circ$/J·K^{-1}·mol^{-1}	ΔS_m°/J·K^{-1}·mol^{-1}	ΔH_m°/J·K^{-1}·mol^{-1}	Φ_m°/J·K^{-1}·mol^{-1}
10	3.90	1.31	9.8	0.326
15	10.88	4.09	45.3	1.068
20	20.45	8.49	122.8	2.343
25	32.53	14.31	254.5	4.132
30	44.90	21.32	447.6	6.400
35	59.92	29.39	710.4	9.096
40	72.95	38.23	1 042	12.18
45	87.53	47.67	1 444	15.59
50	101.66	57.63	1 917	19.30
55	115.43	67.96	2 459	23.25
60	128.26	78.57	3 069	27.41
65	140.40	89.32	3 741	31.76
70	151.38	100.13	4 471	36.26
75	162.04	110.94	5 255	40.88
80	171.99	121.72	6 090	45.59
85	181.38	132.43	6 974	50.39
90	190.55	143.06	7 904	55.24
95	198.71	153.58	8 877	60.14
100	206.26	163.98	9 890	65.07
105	214.84	174.25	10 944	70.03
110	222.01	184.42	12 036	75.00
120	235.86	204.34	14 327	84.95
130	248.89	223.75	16 752	94.88
140	261.31	242.65	19 304	104.76
150	273.49	261.09	21 978	114.57
160	285.22	279.12	24 772	124.30
170	296.97	296.77	27 684	133.93
180	308.85	314.08	30 712	143.45
190	321.35	331.11	33 864	152.88
200	333.88	347.91	37 139	162.22
210	347.23	364.53	40 545	171.46
220	361.12	381.00	44 086	180.61
230	375.60	397.37	47 769	189.67
240	391.05	413.68	51 602	198.67
250	407.08	429.96	55 592	207.59
260	423.14	446.23	59 740	216.46
270	440.77	462.53	64 059	225.27
280	460.36	478.91	68 563	234.04
290	481.89	495.44	73 275	242.77
298.15	500.60	509.04	77 274	249.86
300	504.96	512.15	78 204	251.47
310	532.65	529.46	83 399	260.43
320	575.29	546.98	88 919	269.11
334.5[a,b]	735.27	790.41	169 791	282.81
340	743.88	802.47	173 858	291.13
350	759.00	824.26	181 371	306.05
360	774.30	845.85	189 038	320.75
370	789.65	867.28	196 858	335.23
380	804.96	888.54	204 830	349.51

[a] Extrapolated. [b] Liquid.

Table 6. Measured Enthalpies of Transition and Melting of *n*-Nonadecanol[a]

series	T_{trans}/K	T_{fus}/K	$\Delta H_{trans} + \Delta H_{fus}$/J·mol^{-1}
1	331	334.5	72 516
7	331	334.5	72 319
8	331	334.5	72 434
mean value and estimated error			72 423 ± 100

[a] The following linear fits of the heat capacity were used for the iterative calculation of the baseline: C_p[solid] = {285.92 + 2.63902T} and C_p[liquid] = {227.63 + 1.5176T} J·K^{-1}·mol^{-1}.

peratures, mean heat capacity over the measurement interval, and relative enthalpy values. After calculating starting values for the entropy and enthalpy at 10 K, the data set was interpolated for every degree. The derived properties $S°(T)$ and $\Phi°(T) = -(H°(T) - TS°(T))$ were calculated by numerical integration. The latter function $\Phi°(T)$ is given, as it is useful for calculating relative stabilities and as it is easier to interpolate. The starting values of $S°$ and $H°(T) - H°(0)$ were calculated assuming that below 10 K the low-temperature limit of the Debye heat capacity function $C_p = \alpha T^3$ holds.

Results and Discussion

1-Octadecanol. The experimental data series are given in Table 1. The derived thermodynamic properties $H°(T) - H°(0)$, $S°(T)$, and $\Phi°(T)$ are given in Table 2. All four compounds do not follow the Debye low-temperature limit $C_p = \alpha T^3$ in the temperature range measured. For obtaining starting values for the numerical integration of C_p/T, leading to $S°$, we used the fitted values of C_p at 10 K to calculate α, assuming that below 10 K the Debye limit holds. Between 10 K and just below the melting point, no

Table 7. Experimental Data Series for *n*-Eicosanol

T / K	C_p / J·K^{-1}·mol^{-1}	T / K	C_p / J·K^{-1}·mol^{-1}	T / K	C_p / J·K^{-1}·mol^{-1}	T / K	C_p / J·K^{-1}·mol^{-1}	T / K	C_p / J·K^{-1}·mol^{-1}
series 1		18.57	18.83	80.00	180.43	196.25	346.98	309.92	594.34
295.86	518.89	20.84	23.72	81.96	183.09	198.24	349.82	311.87	605.04
297.11	524.56	23.13	29.39	83.86	188.67	200.23	352.38	313.82	616.96
299.09	530.51	25.49	35.97	85.76	192.44	202.21	355.52	315.77	629.93
301.07	537.75	27.96	41.84	87.69	196.13	204.20	358.00	317.73	647.04
303.05	546.37	30.29	48.31	89.62	199.57	206.19	360.95	319.68	668.29
305.02	554.28	series 3		91.55	203.15	208.17	363.77	321.62	698.55
306.99	563.46	8.14	2.99	93.49	206.51	210.16	366.52	323.54	734.59
308.96	573.17	9.97	4.44	95.43	209.82	212.15	369.63	325.44	786.19
310.92	583.72	11.49	6.19	97.37	213.17	214.13	372.22	327.30	856.66
312.87	596.09	13.35	8.90	99.32	216.10	216.12	375.10	329.11	983.25
314.82	608.17	15.31	12.37	101.05	221.38	218.11	377.96	330.76	1227
316.77	620.89	17.38	16.25	101.93	221.46	220.09	380.83	332.15	1657
318.71	635.10	19.58	20.89	103.36	223.41	222.07	384.12	333.26	2354
320.64	651.05	21.86	26.20	105.33	226.39	224.05	386.81	334.10	3398
322.57	670.46	24.18	32.17	107.28	229.71	226.03	389.71	334.72	4864
324.48	695.70	26.58	38.67	109.24	232.54	228.02	392.75	335.17	6800
326.38	732.86	28.98	44.75	111.20	235.55	230.00	395.90	335.51	9249
328.24	794.81	31.14	50.87	113.16	238.45	231.99	399.36	335.77	12264
330.03	909.58	32.98	56.94	115.12	241.23	233.98	402.12	335.97	15892
331.70	1127	series 4		117.08	244.18	235.96	405.61	336.13	20009
333.16	1671	6.78	1.81	119.05	246.70	237.94	408.77	336.26	24352
334.26	2938	8.63	3.27	121.01	249.41	239.92	412.14	336.37	27929
334.98	5121	10.58	4.90	122.98	252.24	241.90	415.65	336.46	29331
335.44	8233	12.41	7.45	124.95	254.90	243.89	418.70	336.56	27573
335.75	11909	14.58	10.95	126.92	257.91	245.87	422.26	336.68	23378
335.97	15694	16.92	15.26	128.89	260.30	247.85	425.70	336.81	18616
336.15	19533	19.36	20.39	130.86	262.96	249.84	429.35	336.96	18300
336.29	23338	21.94	26.49	132.84	265.40	251.82	433.00	337.10	23342
336.42	27137	24.63	33.46	134.81	268.26	253.80	435.79	337.21	30509
336.53	30494	27.33	40.51	136.78	270.58	255.78	438.83	337.29	39170
336.63	32000	29.77	46.85	138.76	273.17	257.77	442.76	337.36	49113
336.73	30317	31.80	53.07	140.73	275.76	259.75	446.90	337.41	60100
336.84	26011	33.56	58.75	142.71	278.17	261.74	450.69	337.45	72558
336.97	22688	series 5		144.69	281.04	263.72	455.28	337.49	86862
337.10	22853	35.01	63.77	146.67	283.28	265.70	458.95	337.52	94001
337.23	28669	36.33	67.12	148.64	285.77	267.69	462.95	337.55	89777
337.32	37815	37.86	70.80	150.62	288.19	269.67	467.15	337.58	95989
337.40	47645	39.63	76.15	152.60	290.79	271.65	471.61	337.62	78093
337.46	55983	41.38	81.41	154.58	293.51	273.64	475.83	338.21	1847
337.51	86703	43.11	86.71	156.56	296.09	275.62	480.10	339.79	780.06
337.53	297406	44.86	92.01	158.55	299.08	277.60	484.67	341.80	782.58
337.55	128287	46.62	97.28	160.53	301.21	279.59	489.61	343.79	786.29
337.57	138920	48.39	102.48	162.51	303.27	281.57	495.21	345.78	788.77
337.59	436103	50.17	107.65	164.49	305.82	283.55	500.83	347.76	792.08
337.74	9946	51.97	112.73	166.47	308.16	285.53	506.11	349.75	794.69
339.00	778.30	53.77	118.04	168.46	310.61	287.50	511.81	351.73	797.67
341.22	781.21	55.59	123.43	170.44	313.05	289.48	517.92	353.71	800.73
343.31	784.95	57.41	128.30	172.43	315.47	series 6		355.68	802.90
345.30	787.43	59.25	133.18	174.41	318.22	290.72	517.30	357.65	806.01
347.29	790.48	61.10	137.93	176.40	320.54	291.17	519.39	359.61	808.43
349.28	793.43	62.95	142.65	178.38	323.05	292.38	525.48	361.57	811.15
351.27	796.09	64.82	147.15	180.37	325.59	294.33	532.47	363.52	814.58
353.26	799.32	66.69	151.87	182.35	328.10	296.27	539.17	365.48	816.18
355.25	801.89	68.57	156.18	184.34	331.01	298.22	545.42	367.43	818.86
series 2		70.46	160.55	186.32	333.46	300.17	551.71	369.38	821.32
9.78	4.45	72.35	164.82	188.31	336.14	302.12	558.59	371.32	822.98
12.29	7.23	74.25	168.88	190.30	338.66	304.07	567.52		
14.65	11.03	76.16	172.69	192.28	341.64	306.02	574.90		
16.43	14.42	78.07	175.32	194.27	344.20	307.97	584.55		

phase transitions were observed. In the melt the molar heat capacity reaches very high values, and near the end of the melting process when the remaining solid starts to float in the liquid formed, which enhances the distribution of impurities, even negative values for the heat capacity are found. However, this has no influence on the calculation of the enthalpy of fusion. For this calculation, the enthalpy function is used and this function increases with every heat input. In Figure 1 the molar heat capacity in the vicinity of the melting point is given. The first melting experiment showed a very small shoulder; this effect is more pronounced in the once-melted material. The occurrence of a phase transition in the long chain alcohols has been reported, as discussed in the Introduction. The observed effect is attributed to a solid−solid transition, in which the crystalline form is changed into a crystal with rotational disorder. We follow the often-used notation, the β- and γ-forms, which are stable at low temperatures, transform into the α-form at the transition points close to the melting points. On cooling, the compound crystallizes in the α-form. The $\alpha \rightarrow \gamma$ transition (in the case of *n*-octadecanol) does show a significant subcooling. The cooling curve (see the Experimental Section) is given in Figure 2. For all four alcohols the subcooling of the liquid $\rightarrow \alpha$ phase is very small. The temperatures of the freezing process were taken at the point A (see Figure 2) and are given in Table 13. Subcooling ranged from 0.2 K to 0.5 K. The liquid $\rightarrow \alpha$ and $\alpha \rightarrow \gamma$ transitions are clearly separated. The $\alpha \rightarrow \gamma$ transition is a solid−solid phase transition which involves nucleation and which is consequently subcooled. The amount of subcooling depends on the cooling rate. Closer inspection of the thermal plateau (indicated by B in Figure 2) and repeating the cooling curve at different cooling rates showed that what looked to be a first-order phase transition is a balance between the heat liberated by the transition process and the heat removed by the cooling. In Table 3 a summary of the melting experiments is given. The enthalpy of fusion was calculated by taking the enthalpy increment between 300 K and 340 K. The C_p functions of the liquid and the solid used for the calculation of the baseline are also given in Table 3. The calculation was performed in an iterative way, the contribution of the liquid formed being

Table 8. Thermodynamic Properties at Selected Temperatures for *n*-Eicosanol (M = 298.55 g·mol^{-1}, $\Phi_m^\circ \stackrel{def}{=} \Delta_0^T S_m^\circ - \Delta_0^T H_m^\circ/T$)

T	$C_{p,m}^\circ$	ΔS_m°	ΔH_m°	Φ_m°
K	J·K^{-1}·mol^{-1}	J·K^{-1}·mol^{-1}	J·K^{-1}·mol^{-1}	J·K^{-1}·mol^{-1}
10	4.45	1.51	11.3	0.380
15	11.74	4.66	51.1	1.258
20	21.84	9.43	135.0	2.679
25	34.55	15.67	275.9	4.629
30	47.50	23.01	478.3	7.069
35	63.74	31.44	752.5	9.933
40	77.25	40.81	1 104	13.20
45	92.44	50.79	1 529	16.82
50	107.16	61.30	2 028	20.74
55	121.75	72.19	2 600	24.92
60	135.13	83.36	3 242	29.32
65	147.59	94.68	3 950	33.91
70	159.48	106.06	4 718	38.66
75	170.42	117.44	5 543	43.53
80	180.43	128.72	6 417	48.50
85	190.95	139.95	7 343	53.55
90	200.27	151.13	8 322	58.66
95	209.09	162.21	9 346	63.82
100	218.08	173.14	10 413	69.00
105	225.88	184.00	11 526	74.22
110	233.71	194.69	12 676	79.45
120	248.00	215.65	15 086	89.93
130	261.80	236.06	17 636	100.39
140	274.80	255.93	20 319	110.80
150	287.42	275.33	23 131	121.12
160	300.66	294.30	26 072	131.35
170	312.50	312.88	29 136	141.49
180	325.12	331.10	32 324	151.52
190	338.27	349.03	35 642	161.44
200	352.08	366.74	39 094	171.26
210	366.29	384.26	42 687	180.99
220	380.70	401.64	46 422	190.63
230	395.89	418.89	50 305	200.18
240	412.28	436.09	54 346	209.65
250	429.64	453.26	58 554	219.05
260	447.40	470.44	62 934	228.39
270	467.87	487.71	67 510	237.67
280	490.77	505.12	72 300	246.91
290	517.70	522.84	77 348	256.12
298.15	545.19	537.56	81 678	263.61
300	551.16	540.95	82 692	265.31
310	594.75	559.69	88 407	274.50
320	672.60	579.62	94 688	283.72
330	1096	604.37	102 741	293.04
338.2[a,b]	699.6	617.62	106 788	301.86
338.2[a,c]	778.2	835.56	180 494	301.86
340	780.31	839.70	181 898	304.71
350	795.06	862.54	189 775	320.32
360	808.95	885.13	197 797	335.70

[a] Extrapolated. [b] Solid. [c] Liquid.

calculated after each measurement and used in the new calculation until a stable value was obtained. A maximum of three iterations were needed. The sum of the enthalpy of fusion and of transition was found to be (66 672 ± 200) J·mol^{-1}. This is the mean value of four melting experiments; the uncertainty given is two times the standard deviation. It seems that in the compound as received, being stored for a long time at room temperature, lattice defects have healed, resulting in a larger enthalpy of fusion. The difference is within the uncertainty, and it cannot be confirmed by an outlier test that the first melting experiment is different from the following experiments. However, the same effect was observed with all four alcohols. Recent measurements on *n*-heptadecanol showed the same effect, but with this compound the difference in enthalpy of the solid state between the sample as received and after melting amounted to 1000 J·mol^{-1}, which is a significant difference. The temperature of fusion was (331.2 ± 0.1) K, the stated uncertainty is larger than can be expected in adiabatic calorimetry. This is caused by the occurrence of the phase transition in the melting region, which also prohibits the usual purity calculation. An attempt was made to separate the transition and the melting effect. The sample was melted and cooled to 328 K (see Figure 2). At

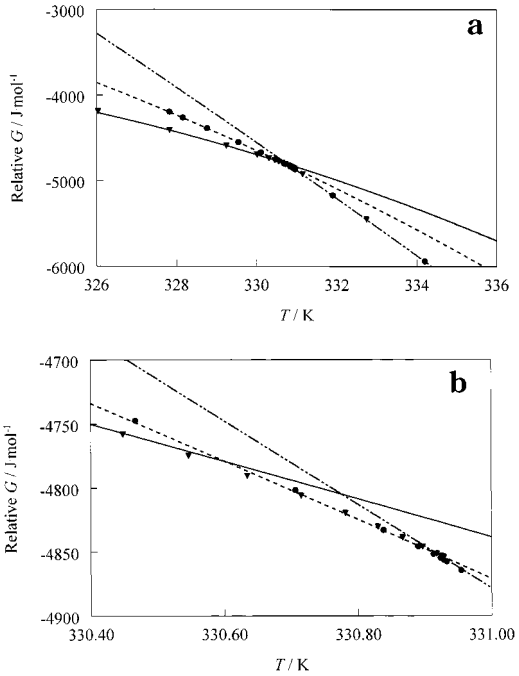

Figure 3. (a) Relative Gibbs energy curves of *n*-octadecanol around the transition and melting point: ▼, compound first cooled to 100 K; ●, compound cooled to 328 K; the region around the transition and melting point is given in part b. (b) Enlarged view of the transition region; the symbols are the same as in part a.

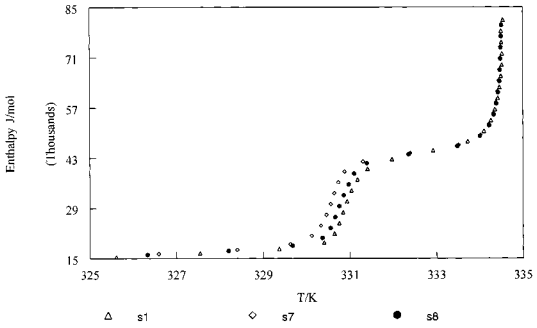

Figure 4. Enthalpy curve of 1-nonadecanol around the melting point; the crystal-rotator transition between 330 K and 331.5 K changes with the thermal history of the sample: Δ, compound as received; +, compound after being melted and slowly cooled; ●, compound after being equilibrated at 332 K for 24 h.

Table 9. Melting Experiments of *n*-Eicosanol[a]

experiment	triple point	ΔH_{fus}	remarks
	K	J·mol^{-1}	
1	338.1	73 968	as received
2	338.2	73 482	
3	338.2	73 706	used in Table 8
mean value		73 719 ± 200	

[a] The following linear fits were used for the iterative calculation of the baseline: C_p[solid] = {−598.07 + 3.8370T} and C_p[liquid] = {310.04 + 1.38521T} J·K^{-1}·mol^{-1}.

this temperature only the liquid → α transition has taken place. From 328 K, set measurements were made up to temperatures in the liquid phase. The molar heat capacities in the (metastable) α-phase were very high. Between 328 K and 330 K the values increased from 1000 to 2000 J·K^{-1}·mol^{-1}. This makes it very difficult to calculate the enthalpy of the α → liquid transition. The difference in enthalpy between the α and the γ phase at 328 K, calculated after matching the enthalpy in the liquid phase, was 25 600 J·K^{-1}·mol^{-1}. Accepting this value as the γ → α enthalpy of transition, thus ignoring the heat capacity contribution, the enthalpy of fusion of the α phase is 41 072

Table 10. Experimental Data Series for *n*-Docosanol

T/K	C_p/J·K^{-1}·mol^{-1}	T/K	C_p/J·K^{-1}·mol^{-1}	T/K	C_p/J·K^{-1}·mol^{-1}	T/K	C_p/J·K^{-1}·mol^{-1}	T/K	C_p/J·K^{-1}·mol^{-1}
series 1		357.98	879.57	65.26	160.24	189.56	366.95	291.13	553.77
296.30	564.01	360.28	883.20	67.12	164.92	192.51	371.12	294.07	562.12
298.36	570.12	series 2		68.98	169.67	195.46	375.56	297.02	570.47
301.19	578.80	5.46	0.80	70.85	174.53	198.41	379.85	299.97	579.47
304.01	587.73	7.96	2.42	72.73	179.06	201.37	384.41	302.91	589.11
306.80	597.02	10.53	4.64	74.62	184.08	204.32	388.63	305.85	598.60
309.57	606.84	11.91	5.41	76.51	188.66	207.28	393.06	308.80	608.87
312.32	616.97	13.78	9.34	78.41	192.96	210.23	397.61	311.74	618.06
315.05	627.29	15.59	12.67	80.32	197.46	213.19	402.07	314.69	627.04
317.76	638.53	17.49	16.68	82.23	201.41	216.15	406.79	317.63	637.21
320.45	650.17	19.64	21.68	84.14	205.41	219.10	411.48	320.57	649.18
323.11	662.51	21.88	27.26	86.06	209.34	222.06	416.03	323.51	662.56
325.76	676.88	24.20	33.61	87.98	213.68	225.02	420.88	326.44	678.59
328.38	694.27	26.61	40.53	89.90	217.48	227.97	425.87	329.36	699.34
330.97	716.13	29.11	48.12	91.83	221.28	230.93	430.63	332.26	729.87
333.52	746.90	series 3		93.76	223.95	233.88	435.55	335.11	786.21
336.00	806.19	6.98	1.10	95.70	228.53	236.84	440.66	337.85	931.97
338.30	984.55	8.98	3.05	97.63	232.36	239.80	445.90	340.19	1508
340.26	1446	10.62	4.81	99.57	235.99	242.75	451.10	341.76	3746
341.62	3157	12.25	6.06	series 5		245.71	456.42	342.56	9262
342.35	7276	14.21	10.02	106.35	247.64	248.67	461.75	342.94	17842
342.73	13008	16.00	13.52	109.93	253.55	251.62	467.18	343.16	30107
342.96	19841	17.94	17.65	113.42	259.18	254.58	472.72	343.29	46643
343.12	28576	20.12	22.80	116.85	264.65	257.53	478.41	343.38	69267
343.23	42225	22.36	28.57	120.21	269.80	260.49	484.23	343.45	71341
343.31	62840	24.71	35.08	123.52	274.82	263.45	490.20	343.51	92401
343.36	85106	27.14	41.97	126.77	279.71	266.40	496.25	343.56	122013
343.41	79785	29.66	49.82	129.97	284.47	269.36	501.94	343.60	151663
343.46	78818	series 4		133.13	289.01	272.32	508.70	343.63	187689
343.50	91328	32.25	58.11	136.24	293.25	275.28	514.85	343.65	231870
343.54	106619	34.72	66.14	139.31	297.60	278.24	521.53	343.67	269040
343.57	124827	36.86	73.02	142.34	301.79	281.19	528.46	343.69	252897
343.60	153361	38.76	79.23	145.35	305.99	284.14	535.35	343.71	213052
343.62	187971	40.48	85.04	148.32	310.07	287.07	542.67	343.74	166636
343.64	250216	42.14	90.59	151.27	314.06	289.98	550.25	343.78	79277
343.66	325526	43.83	95.84	154.21	318.11	292.87	558.04	344.89	1530
343.67	318848	45.54	101.44	157.15	322.05	295.74	566.10	347.47	864.08
343.68	234220	47.27	106.98	160.08	326.01	298.59	573.42	350.48	868.92
343.70	196166	49.01	112.56	163.02	330.07	series 6		353.47	873.71
343.72	154618	50.77	117.90	165.97	334.04	268.58	499.63	356.45	878.34
343.76	69503	52.54	123.42	168.91	338.13	270.83	504.74	359.43	882.69
344.50	1932	54.32	128.75	171.85	342.18	273.43	510.94	362.40	887.04
346.38	862.90	56.12	134.43	174.80	346.29	276.38	517.37	365.36	891.39
348.71	865.14	57.93	139.45	177.75	350.31	279.33	524.25	368.31	895.29
351.03	868.52	59.75	144.75	180.70	354.51	282.28	531.43	371.25	899.04
353.35	872.26	61.58	149.76	183.65	358.47	285.23	538.97		
355.67	876.03	63.41	155.13	186.60	362.76	288.18	546.53		

J·K^{-1}·mol^{-1}. The relative Gibbs energy curves were calculated for the measurement from the $\gamma \rightarrow \alpha \rightarrow$ liquid and the $\alpha \rightarrow$ liquid measurements. The enthalpy and the entropy of the three data sets were matched at 350 K. The result is plotted in Figure 3a. The transition from the $\gamma \rightarrow \alpha$ phase is very close to the melting point of the α phase. In Figure 3b an enlarged view of the transition region is given. Using the extrapolated Gibbs energy curves (the lines in Figure 3a), we found $T_{\gamma \rightarrow \alpha} = 330.60$ K and $T_{\alpha \rightarrow \text{liquid}} = 330.93$ K. This latter value corresponds to the melting point (see Table 1); this indicates that the extrapolation of the Gibbs energy curves can be used. As this extrapolation is based on measurements relatively far from the melting point, the influence of impurities in the sample is expected to be small. The triple point (331.2 K) was estimated from the plot of the reciprocal of the melted fraction against the equilibrium temperatures.

1-Nonadecanol. The experimental data are given in Table 4, the derived thermodynamic properties are given in Table 5, and the enthalpy of transition and of melting is given in Table 6. The separation of the crystal-rotator transition and the rotator-liquid transition is about 4 K. The molar heat capacity between these transitions is very high and resembles the behavior in *n*-nonadecane.[16] Since it is not clear which baseline to use when trying to separate these transitions, the sum of them is given. The transition temperature shifted slightly to lower temperatures when the sample had been melted before. We stabilized the sample at 332 K, between the transition and the melting point for 24 h and recooled. The different enthalpy curves are given in Figure 4. The stabilization at 332 K resulted in a shift of the transition temperature roughly between the two other curves. This also confirms the idea that storage of the material at room temperature can lead to a slightly different enthalpy of the solid phase. The cooling curve from the liquid phase will be discussed later on.

1-Eicosanol. The experimental data are given in Table 7, the derived thermodynamic properties are given in Table 8, and the melting experiments are given in Table 9. Like the molar heat capacity curve of 1-octadecanol, a small shoulder was observed in the melting curve at about 1 K below the end melting point. The position of the maximum of this effect shifted about 0.2 K to lower temperatures in a sample which had recently been melted. The melting experiments given in Table 9 include this effect. The controlled cooling curve gave two well-separated transitions. This will be discussed in a later section.

1-Docosanol. The experimental data are given in Table 10, the derived thermodynamic properties are given in Table 11, and the melting data are given in Table 12. No solid−solid phase transitions were observed. In the melt only one measuring point could indicate a small transition. Plotting the equilibrium temperatures in the melt versus the reciprocal of the melted fraction does result in a straight line. This indicates that the impurities form a eutectic system with the main component. From these curves the purity and the triple-point temperature given in Table 12 were calculated.

Cooling Behavior. All four compounds do show two events on cooling. A cooling curve of 1-octadecanol is given

Table 11. Thermodynamic Properties at Selected Temperatures for *n*-Docosanol (M = 326.61 g·mol^{-1}, $\Phi_m^\circ \stackrel{def}{=} \Delta_0^T H_m^\circ/T$)

T	$C_{p,m}^\circ$	ΔS_m°	ΔH_m°	Φ_m°
K	J·K^{-1}·mol^{-1}	J·K^{-1}·mol^{-1}	J·K^{-1}·mol^{-1}	J·K^{-1}·mol^{-1}
10	3.92	1.310	9.8	0.330
15	11.50	4.055	44.9	1.057
20	22.51	8.833	129.2	2.369
25	35.92	15.29	275.1	4.286
30	50.89	23.13	491.1	6.761
35	67.03	32.12	783.4	9.732
40	83.43	42.05	1 156	13.14
45	99.69	52.82	1 614	16.95
50	115.59	64.16	2 153	21.10
55	130.89	75.89	2 769	25.54
60	145.46	87.91	3 461	30.24
65	159.57	100.11	4 223	35.14
70	172.31	112.40	5 053	40.22
75	185.03	124.72	5 946	45.44
80	196.76	137.03	6 900	50.78
85	207.17	149.27	7 910	56.22
90	217.67	161.42	8 972	61.72
95	226.92	173.43	10 083	67.29
100	236.75	185.33	11 243	72.89
105	245.38	197.09	12 449	78.53
110	253.67	208.69	13 696	84.18
120	269.48	231.43	16 311	95.51
130	284.50	253.60	19 081	106.82
140	298.56	275.19	21 996	118.08
150	312.34	296.26	25 051	129.26
160	325.90	316.85	28 242	140.34
170	339.63	337.02	31 569	151.32
180	353.51	356.83	35 035	162.19
190	367.58	376.31	38 640	172.95
200	382.30	395.54	42 388	183.60
210	397.26	414.55	46 286	194.14
220	412.87	433.39	50 335	204.59
230	429.13	452.10	54 545	214.94
240	446.26	470.71	58 920	225.21
250	464.18	489.29	63 472	235.41
260	483.25	507.87	68 208	245.53
270	503.16	526.48	73 140	255.59
280	525.79	545.18	78 284	265.60
290	550.31	564.05	83 662	275.56
298.15	572.58	579.62	88 239	283.66
300	579.57	583.22	89 316	285.50
310	612.67	602.76	95 276	295.42
320	646.74	622.71	101 563	305.33
330	704.84	643.40	108 287	315.26
340	1453	669.20	116 941	325.25
343.92[a,b]	681	674.9	118 753	329.61
343.92[a,c]	859.46	925.36	204 892	329.61
350	868.15	935.51	208 423	340.02
360	883.53	960.19	217 184	356.90

[a] Extrapolated. [b] Solid. [c] Liquid.

Table 12. Melting Experiments of *n*-Docosanol[a]

experiment	triple point	ΔH_{fus}	purity	remarks
	K	J·mol^{-1}	%	
1	343.92	86 072	98.3	as received
2	343.92	85 964	98.3	
3	343.90	86 071	98.3	
4	343.92	86 139	98.4	used in Table 8
mean value		86 062 ± 100	98.3	

[a] The following linear fits were used for the iterative calculation of the baseline: C_p[solid] = {−150.62 + 2.418T} and C_p[liquid] = {352.18 + 1.475T} J·K^{-1}·mol^{-1}.

in Figure 2. The temperatures indicated by A and B in the figure are the maximum values measured on each plateau. In Table 13 these values are given. The maximum difference in the solid−liquid and liquid−solid transitions is 0.5 K. One should however be cautious to consider this as subcooling, as different solid phases are involved. 1-Docosanol might melt from the γ phase, and it does crystallize in the α phase. This can account for the difference in the melting and crystallization temperatures. In the case of the *n*-alkanes the subcooling is smaller for compounds with comparable chain lengths; for *n*-nonadecane we measured only 0.1 K or less.[16] The subcooling of the rotator-crystal phase transition is much larger. It ranges between 5 and

Table 13. Comparison of the Experimental and Literature Data

compd	T_{trans}	T_{fus}	ΔH_{trans}	ΔH_{fus}	$\Delta H_{trans} + \Delta H_{fus}$	ref
	K	K	J·mol^{-1}	J·mol^{-1}	J·mol^{-1}	
octadecanol		331.65				10
	328.45	331.65	18 828	39 162	57 990	4
	330	331	26 000	43 000	69 000	3
	327.85	331.75				8
	325.15	330.15				7
	330.25	331.55				9
		330.85				11
		331.95				12
	325.1[a]	330.49[a]	22 300	37 300	59 600	1
	326.1[a]	330.7[a]				this work
	330.60	331.2	25 600	41 072	66 672	this work
nonadecanol		335.15				7
		334.65				11
		335.15				12
	324.55	334.2	23 800	42 600	66 400	1
	326.3[a]	334.0[a]				this work
	331	334.5			72 423	this work
eicosanol		338.15				7
	335.05	338.05				9
	337.65	343.55	13 933	41 840	62 073	4
		338.15				12
	331.45[a]	337.58[a]	24 400	45 700	70 100	1
	329.7[a]	337.3[a]				this work
		338.2			73 719	this work
docosanol	340.15	345.15				7
	343.95	348.05	17 238	46 568	63 806	4
		343.65				12
	336.65[a]	343.1[a]	26 200	51 040	77 240	1
	339.8[a]	343.2[a]				this work
		343.92			86 062	this work

[a] Cooling.

7 K, and whereas the crystallization temperatures measured by Sirota[1] are in accord with our measurements, the transition temperatures differ up to 3 K. Since the cooling rates were comparable in both works, the cause of the difference could be the material of the measuring vessels. This would indicate that the transition is triggered by nonhomogeneous nucleation.

Entropy at 360 K and 298.15 K. We fitted the entropy $S°$(360 K) for the four components in the liquid phase to a function of the form $S° = a_0 + a_1 n$, where n is the number of carbon atoms in the chain. The value of $S°$(360 K) = 806.83 J·K^{-1}·mol^{-1} of 1-octadecanol was calculated by extrapolation from 350 K using the fit for the liquid phase (see later discussion). The fit obtained is $S°$(360 K,n) = {117.52 + 38.328n} J·K^{-1}·mol^{-1}, with a correlation coefficient of 0.999 93. The maximum deviation from the fit is found for 1-nonadecanol and is 0.11%, which is within the expected accuracy. The increment in entropy with n can be compared with the value given for the *n*-alkanes. The fit at 298.15 K of these compounds gives a value of 32.32 J·K^{-1}·mol^{-1}.[17] When we extrapolate the entropy of the alcohols to a hypothetical liquid state at 298.15 K, by using the fit of the heat capacity of the liquid phases as described later on, we find $S°$(298.15,n) = {111.31 + 31.448n} J·K^{-1}·mol^{-1}. The maximum deviation in this fit is 0.18% for 1-docosanol. The dependence of $S°$ on n is close to the value found for the *n*-alkanes.

Heat Capacity of the Liquid Phase. We have combined all collected heat capacity data of the liquid phase of the four compounds in a file consisting of *temperature−number of carbon atoms−heat capacity* triplets. With these data a fit was made, starting with the model $C_p = a_0 + a_1 n + a_2 nT + a_3 T$. The program Exel with the Solver option was used for the fitting procedure. This model allows for a change in temperature dependence of the heat capacity of the liquids with the carbon number. However, it proved to be possible to fit the data set to within the experimental error and with the same error as in the aforementioned fit, with the more simple function $C_p = a_0 + a_1 n + a_2 T$. A total number of 157 data points were used, giving the

function $C_p = \{-450.41 + 36.4968n + 1.47317T\}$ J·K^{-1}·mol^{-1}. The standard deviation of this fit is 0.7 J·K^{-1}·mol^{-1}, which corresponds to a relative deviation of about 0.1%. This fit shows that the heat capacity of the liquids of the four alcohols has the same temperature dependence. No explanation has been made at the time of this writing.

Acknowledgment

The authors wish to thank the students Edwin de Heer (Utrecht University) and Cathal Brennan (Trinity College, Dublin) for assisting in the measurements.

Literature Cited

(1) Sirota, E. B.; Wu, X. Z. The Rotator Phase of Neat and Hydrated 1-Alcohols. *J. Chem. Phys.* **1996**, *105*, 7763−773.

(2) Yamamoto, T.; Nozaki, K.; Hara, T. X-ray and Thermal Studies of Normal Higher Alcohols $C_{17}H_{35}OH$, $C_{18}H_{37}OH$, and Their Mixtures. *J. Chem. Phys.* **1990**, *92*, 631−641.

(3) Reuter, J.; Würflinger, A. Differential Thermal Analysis of Long-Chain *n*-Alcohols Under High Pressure. *Ber. Bunsen-Ges. Phys. Chem.* **1995**, *99*, 1247−1251.

(4) Kuchal, Y. K.; Shukla, R. N.; Biswas, A. B. Differential Thermal Analysis of *n*-Long Chain Alcohols and Corresponding Alkoxy Ethanols. *Thermochim. Acta* **1979**, *31*, 61−70.

(5) Mosselman, C.; Mourik, J.; Dekker, H. Enthalpies of Phase Change and Heat Capacities of Some Long-chain Alcohols. Adiabatic Semi-Microcalorimeter for Studies of Polymorphism. *J. Chem. Thermodyn.* **1974,** *6*, 477−487.

(6) Hoffman, J. D.; Smyth, C. P. Molecular Rotation in the Solid Forms of Some Long-Chain Alcohols. *J. Am. Chem. Soc.* **1949**, *71*, 431−439.

(7) Tanaka, K.; Seto, T.; Hayashida, T. Phase Transformation of *n*-Higher Alcohols. (I) *Bulletin Institute Chemical Research Kyoto University* **1958**, *35* 123−139.

(8) Kolp, D. G.; Lutton, E. S. The Polymorphism of *n*-Hexadecanol and *n*-Octadecanol. *J. Am. Chem. Soc.* **1951**, *73*, 5593−5595.

(9) Pradhan, S. D.; Katti, S. S.; Kulkarni, S. B. Dielectric Properties of *n*-Long Chain Alcohols, Alkoxyethanols and Alkoxypropanols. *Ind. J. Chem.* **1970**, *8*, 632−637.

(10) Smith, J. C. Higher Aliphatic Compounds. Part I. The Systems Ethyl Pamitate-Ethyl Stearate and Hexadecyl Alcohol-Octadecyl Alcohol. *J. Chem. Soc.* **1931**, 802−807.

(11) Gaikwad, B. R.; Subrahmanyam, V. V. R. Melting Behaviour of Fatty Alcohols and Their Binary Blends. *J. Ind. Chem. Soc.* **1985**, *LXII*, 513−515.

(12) Tasumi, M.; Shimanouchi, T.; Watanabe, A.; Goto, R. Infrared Spectra of Normal Alcohols-I. *Spectrochim. Acta* **1964**, *20*, 629−666.

(13) Small. D. M. *Handbook of Lipid Research 4, The Physical Chemistry of Lipids*; Plenum Press: New York, 1988.

(14) van Miltenburg, J. C.; van den Berg, G. J. K.; van Bommel, M. J. Construction of an Adiabatic Calorimeter. Measurement of the Molar Heat Capacity of Synthetic Sapphire and of *n*-Heptane. *J. Chem. Thermodyn.* **1987**, *19*, 1129−1137.

(15) van Miltenburg, J. C.; van Genderen, A. C. G.; van den Berg, G. J. K. Design Improvements in Adiabatic Calorimetry. The Heat Capacity of Cholesterol Between 10 and 425 K. *Thermochim. Acta* **1998**, *319*, 151−162.

(16) van Miltenburg, J. C.; Oonk, H. A. J.; Metivaud, V. Heat Capacities and Derived Thermodynamic Functions of *n*-Nonadecane and *n*-Eicosane Between 10 K and 390 K. *J. Chem. Eng. Data* **1999**, *44*, 715−720.

(17) Messerly, J. F.; Guthrie, G. B.; Todd, S.; Finke, H. L. Low-Temperature Thermal Data for *n*-Pentane, *n*-Heptadecane, and *n*-Octadecane. *J. Chem. Eng. Data* **1967**, *12*, 338−346.

Received for review February 8, 2000. Accepted October 24, 2000.

JE000048S